Quantitative Investigation of Heat-Affected Zone Cracking in Aluminum Alloy A6061

Grain size, solidus temperature and concentrations of Si and Mg were studied as factors influencing HAZ cracking

BY M. MIYAZAKI, K. NISHIO, M. KATOH, S. MUKAE AND H. W. KERR

ABSTRACT. The influences of several factors on heat-affected zone cracking of aluminum Alloy A6061 were investigated. First, the influence of the grain size on the weld heat-affected zone cracking of GTA spot welds on A6061 was studied using a Varestraint test. The maximum crack length increased when the grain size was increased from 0.05 to 2 mm, but increased more gradually for further increases in grain size. The influences of solidus temperature and penetration of alloying elements from the weld metal into the HAZ were investigated for GMA welds. For dilutions between 20 and 80%, for both 5356 and 4043 filler metals, the solidus temperature was increased by Si, but decreased by Mg. Generally, the solidus was higher in the case of 5356 filler metal. Longitudinal cracking was developed along the fusion boundary only in the case of 5356 filler metal. This phenomenon was explained using the relation between the solidus temperature and the heat input. Transverse cracking was observed for the welded condition using 4043 filler metal, but in the case of 5356 filler metal, subsurface cracks developed, and were observed only after machining-off the reinforcement. High concentrations of Si and Mg were observed near cracks in the case of 4043 and 5356 filler metals, respectively. This indicates that penetration of these elements affects the transverse cracking.

Introduction

Al-Mg-Si alloys have been widely used in welded structures. Anticorrosion treatment is almost unnecessary for these alloys even near a beach, because they have good corrosion resistance. The proof stress of A6061-T6 is defined to be more than 250 MPa (36 ksi); almost the same as the yield stress of a mild steel. These alloys have, however, higher crack susceptibilities than mild steel in the weld heat-affected zone.

Previous work has been reported concerning this HAZ cracking. For example, Tsujimoto, *et al.*, has performed studies using GMA welding. He reported that cracks could be developed due to the invasion of low-melting compounds and/or the diffusion of Mg and Si from the weld metal along grain boundaries in the HAZ (Ref. 1).

Moreover, Gittos, *et al.*, performed a study using the Patch test, and reported that longitudinal cracking was developed when the solidus temperature of the weld metal was higher than that of the base metal (Ref. 2). These results are all qualitative. Katoh and Kerr have performed a quantitative study on Al-Mg-Si alloys using the Varestraint test (Refs. 3, 4). The main results obtained are as follows: liquation cracks were developed in the HAZ of the weld metal with GTA welding, and both augmented strain and heat input larger than critical values were necessary for the cracks to be developed. In the case of an extruded material in which the grain size was larger than in the case of a rolled material, the crack length tended to become longer even for the same heat input and augmented strain. The crack susceptibility in GTA welding was decreased by alloying elements such as Cr, Mn and Cu, but was increased by Mg and Si. With GMA welding, both longitudinal and transverse cracks were developed in the HAZ when 5356 filler metal was used. Only transverse cracks were developed when 4043 filler metal was used. Generalizing these results, it is considered that the following three factors will affect the development of a crack: 1) thermal factor, heat necessary to melt grain boundaries; 2) metallurgical factor, crack susceptibility of a material; and 3) mechanical factor, force or deformation necessary to open grain boundaries.

KEY WORDS

Aluminum Alloy A6061
A6061 HAZ Cracking
Quantitative Study
5356 Filler Metal
4043 Filler Metal
Effect of Mg Addition
Effect of Si Addition
Solidus Temp. Effect
Liquation Cracking
GTA Spot/GMA Welding

There are still many factors which have not yet been investigated in detail. The present investigation was made first on the influence of the grain size using a Varestraint test when GTA welding was performed. The influences of solidus temperature and penetration of alloying elements from weld metal into the HAZ were also investigated.

Materials Used and Experimental Procedures

Table 1 shows the chemical compositions of the materials used. Commercial A6061-0 alloy, which was obtained by annealing A6061-T6 listed in Table 1, was used to investigate the influence of grain size, and the commercial A6061-T6 alloy was used to examine other aspects. Dimensions of the test specimens were 6 mm (0.24 in.) thick, 50 mm (2 in.) wide and 110 mm (4.3 in.) long.

Grain sizes of the base metal were changed using the strain-annealing method. That is, the base metals were annealed in air for 15 h at 590°C (1094°F) after being tensile strained between 2 and 30%. The largest average grain size of about 9 mm (0.35 in.) was obtained in the case of tensile strain of about 4%. When tensile strains were larger than 4%, average grain sizes decreased hyperbolicly with increases in tensile strain. An average grain size of about 0.5 mm (0.02 in.) was obtained for a tensile strain of 20%. Little coarsening of grain size was obtained for

M. MIYAZAKI, K. NISHIO, M. KATOH and S. MUKAE are with the Department of Materials Science and Engineering, Kyushu Institute of Technology, Kitakyushu, Japan. H. W. KERR is with the Department of Mechanical Engineering, University of Waterloo, Waterloo, Ontario, Canada.

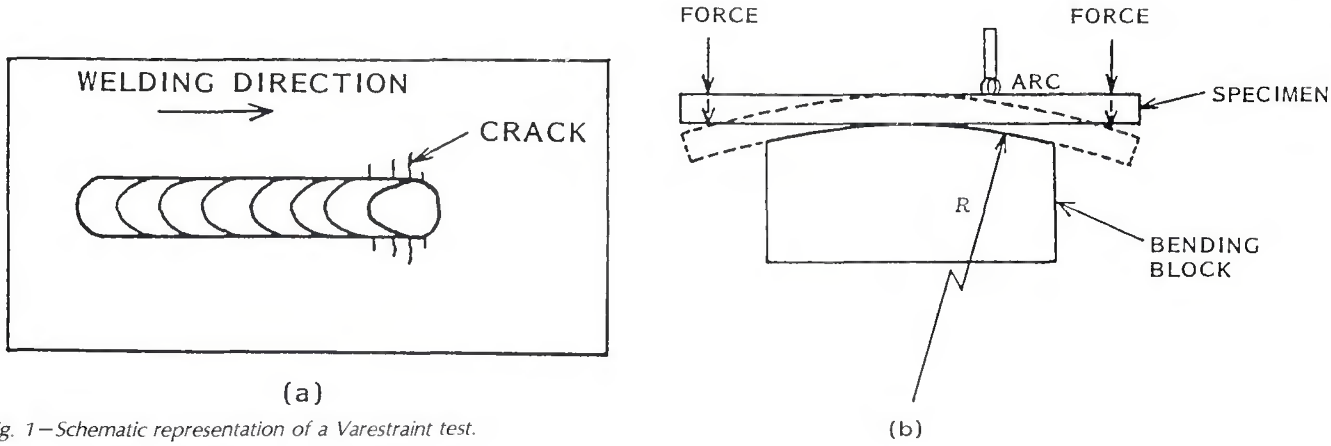

Fig. 1 — Schematic representation of a Varestraint test.

tensile strains less than 4%, for which the average grain sizes were between 0.05 mm (0.002 in.) and 0.2 mm (0.008 in.) (the grain size of the base metal of A6061-0 being about 0.05 mm).

The susceptibility to liquation cracking was evaluated by the maximum crack length that was observed in the HAZ when a Varestraint test was performed. Figure 1 shows a schematic representation of a Varestraint test. GTA spot welding was performed for the study on the influence of grain size, and GMA welding was performed for the others. In order to change the augmented strain, seven bending blocks were employed having radii R between 75 mm (3 in.) and 1000 mm (39 in.). The augmented strain ϵ was obtained using Equation 1:

$$\epsilon = t/2R \qquad (1)$$

where t is the thickness of the specimen. A ram speed of 35.3 mm/s (1.4 in./s) was used for this investigation because little difference in the crack length was observed when preliminary tests were performed using ram speeds of 22.4, 30.0 and 35.3 mm/s (0.9, 1.2 and 1.4 in./s).

GTA spot welding was performed in the center of a specimen under the conditions of welding current I = 120 A, arc voltage E = 25 ~ 28V and arc time t = 20 s (DCEP). The conditions of GMA welding were I = 140 A and E = 21~23 V. Welding heat inputs were changed by changing welding speeds between 200 and 1300 mm/min (8 and 51 in./min). When performing a Varestraint test, bead-on-plate welds were deposited along the centerline of the specimen in the longitudinal direction. The specimen was bent approximately one second before the arc for the welding was stopped.

The crack lengths were measured using a projector (20X) or a magnifying glass eyepiece (the minimum scale: 0.1 mm) in the as-welded condition in the case of GTA spot welding. For GMA welds, the lengths of the longitudinal and transverse cracks were measured after the reinforcement was removed by machining.

Table 1—Chemical Compositions of Materials Used (wt-%)

	Si	Cu	Fe	Mg	Mn	Zn	Cr	Ti
Commercial 6061-T6	0.550	0.170	0.264	0.890	0.018	0.010	0.105	0.038
4043 filler metal	4.770	0.006	0.100	0.010	0.030	0.007	0.037	0.041
5356 filler metal	0.020	0.008	0.088	4.880	0.058	0.005	0.053	0.075

Study of GTA Welds

Relation between Grain Boundaries and Features of Cracks

Figures 2A–C schematically show cracks that were observed in the HAZ when GTA spot welding was performed on the T6 base metal and annealed materials with coarse grains. Figure 2 A was the result for the base metal, in which cracks were developed radially in the HAZ. The crack length was the longest in the direction of Θ = 0 deg and decreased with an increase in theta as indicated in Fig. 2A (Ref. 4). Figure 2B was the result in coarse-grained material when there were two grain boundaries near the weld metal; cracks propagated along these grain boundaries. Thus, the cracks observed here were intergranular. Therefore, when there was no grain boundary, no crack was observed even in the direction of Θ = 0 deg, which is the easiest direction for the cracks to develop (Ref. 4). Figure 2C was the result when there were parallel lamellar grain boundaries in the direction of Θ = 0 deg. Cracks were observed along these grain boundaries. The same orientation of cracks, normal to the maximum tensile strain, was observed even in the direction of Θ being nearly 90 deg, where no crack was observed in the case of the base metal. As shown in Fig. 2C, the crack length increased from Θ = 0 to Θ = 90 deg in this case, since the contour of each crack end and the fusion boundary of the weld metal were nearly in a concentric configuration as indicated by the thin solid line in this figure. This phenomenon supports the result that the liquation-cracked region has a close relation with the maximum temperature in the HAZ, to be discussed later.

Influence of Grain Size on the Maximum Crack Length

Figure 3 shows the relation between the maximum crack length and grain size

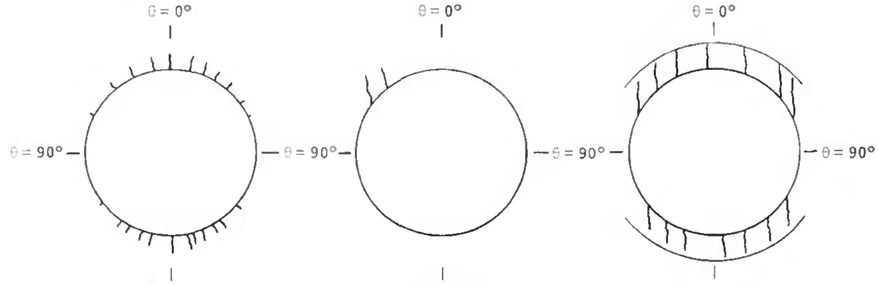

Fig. 2 — Schematic representation of HAZ cracking. A — In the case of base metal; B — in the case of having two grain boundaries; C — in the case of having lamellar grain boundaries.

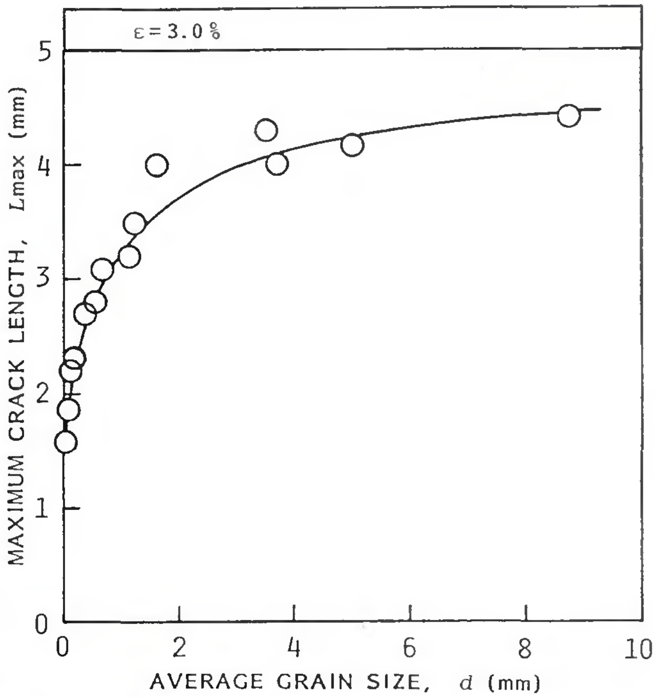

Fig. 3 — Relation between the maximum crack length and average grain size (ϵ = 3.0%).

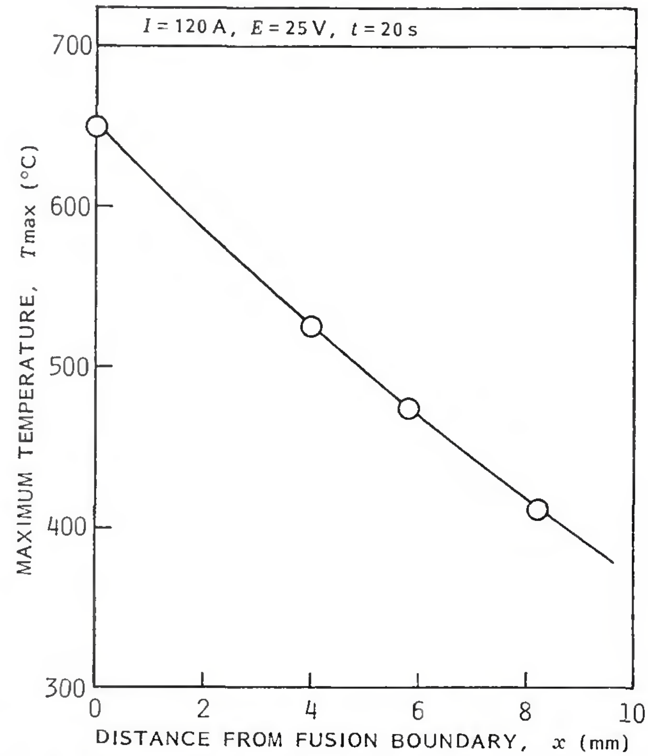

Fig. 4 — Relation between the distance from the fusion boundary into HAZ and the maximum temperature.

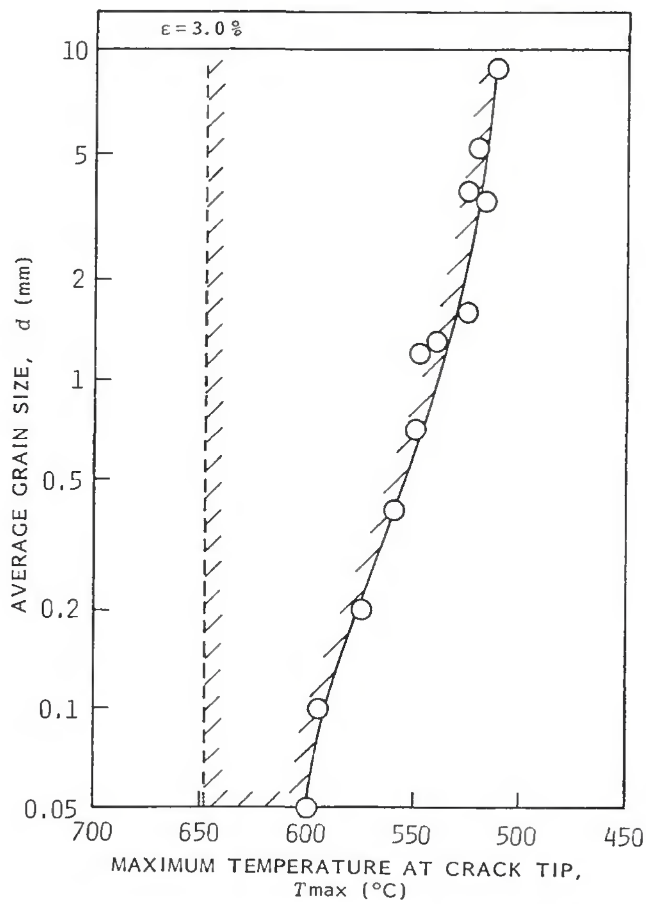

Fig. 5 — Relation between the logarithm of grain size and the maximum temperature at the crack tip.

d for a fixed augmented strain. The maximum crack length (the maximum radial distance of cracking from the fusion boundary) increased greatly for grain sizes between 0.05 and 2 mm (0.002 and 0.08 in.), but increased more gradually with further increases in the grain size above 2 mm. The maximum crack length reached up to 4.5 mm (0.2 in.) when the grain size was 8.8 mm (0.35 in.). Figure 4 shows the relation between the distance from the fusion boundary into the HAZ and the maximum temperature, as measured by temperature-indicating lacquers. The relation between the grain size effect and the maximum temperature of cracking is shown in Fig. 5, which can be obtained by combining Figs. 3 and 4. In the case of the base metal, the maximum temperature was 600°C (1112°F) at the crack tip. This is almost the same as the measured solidus temperature (597°C/1107°F) of the base metal. When the grain size became larger, the maximum temperature at the crack tip gradually decreased and cracks were observed even at temperatures much lower than the solidus temperature of the base metal. For the largest grain size studied, 8.8 mm, the maximum temperature at the crack tip was 513°C (955°F).

Figure 6 shows fractographs of the base metal and the material of d = 8.8 mm. The maximum temperatures of each fractograph obtained using Fig. 4 are 620°C (1148°F) and 530°C (986°F). In Fig. 6A, the fractograph shows clearly that the crack surface was partly melted. In Fig. 6B, however, a flat region is mainly observed with less irregularities.

Study of GMA Welds

Longitudinal Crack

When GMA welding is performed, features of the development of the cracks depend on the filler metals employed (Ref. 3). Only transverse cracking is developed in the case of 4043 filler metal. In the case of 5356 filler metal, however, longitudinal cracking, which is along the partially melted zone near the fusion boundary as shown in Fig. 7, is also developed besides the transverse cracking. Two of the authors already have reported this phenomenon (Ref. 3). A further investigation of longitudinal cracking was made, paying attention to the changes of the solidus temperature when the heat input was changed.

Influence of Heat Input and Augmented Strain

Figures 8A and B show the relations between the crack length L and the heat input Q (kJ/cm), and between the crack length and augmented strain ϵ, respectively. The crack began to develop when the heat input was greater than 2 kJ/cm and increased initially linearly with an increase in the heat input. The slope of the crack length vs. the heat input tended to decrease when the heat input was greater than 7 kJ/cm. No crack was observed for an augmented strain of 1.0%. When the augmented strain became larger than 1.0%, the crack length tended to increase with an increase in the augmented strain. Molten regions were clearly observed on the crack surface near the molten

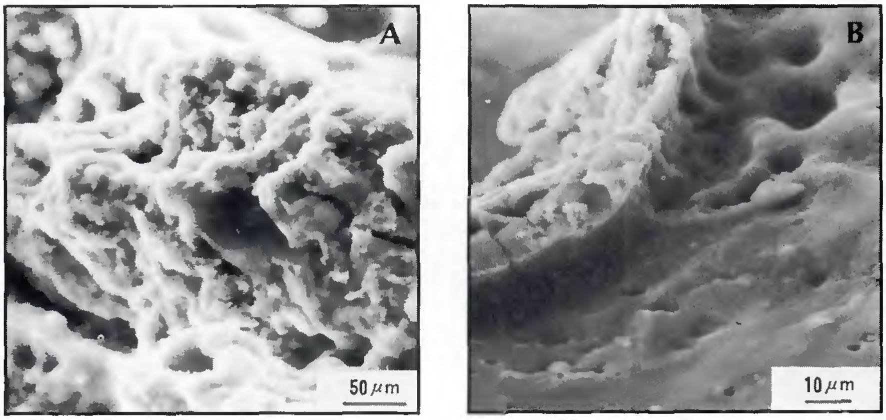

Fig. 6 — Examples of fractographs of fracture surface. A — In the case of base metal; B — in the case of grain size of 8.8 mm.

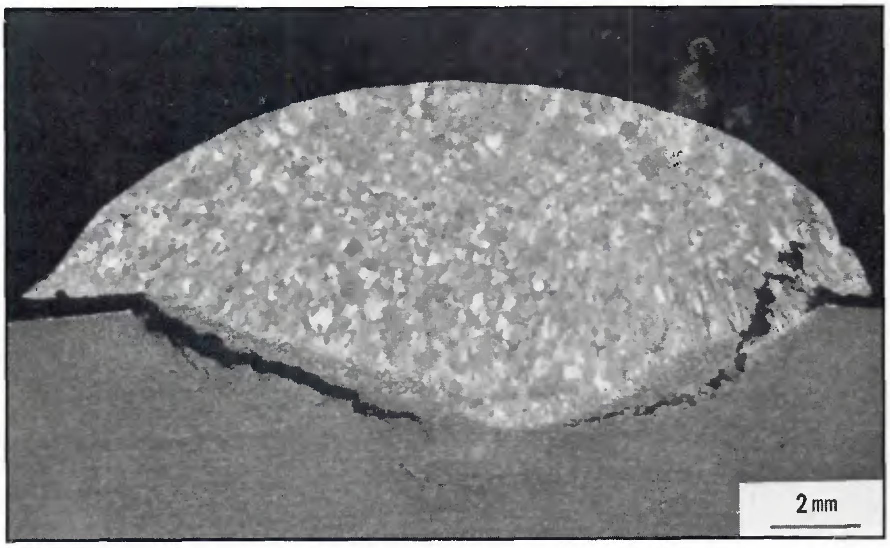

Fig. 7 — Macro structure of the cross-section of longitudinal crack.

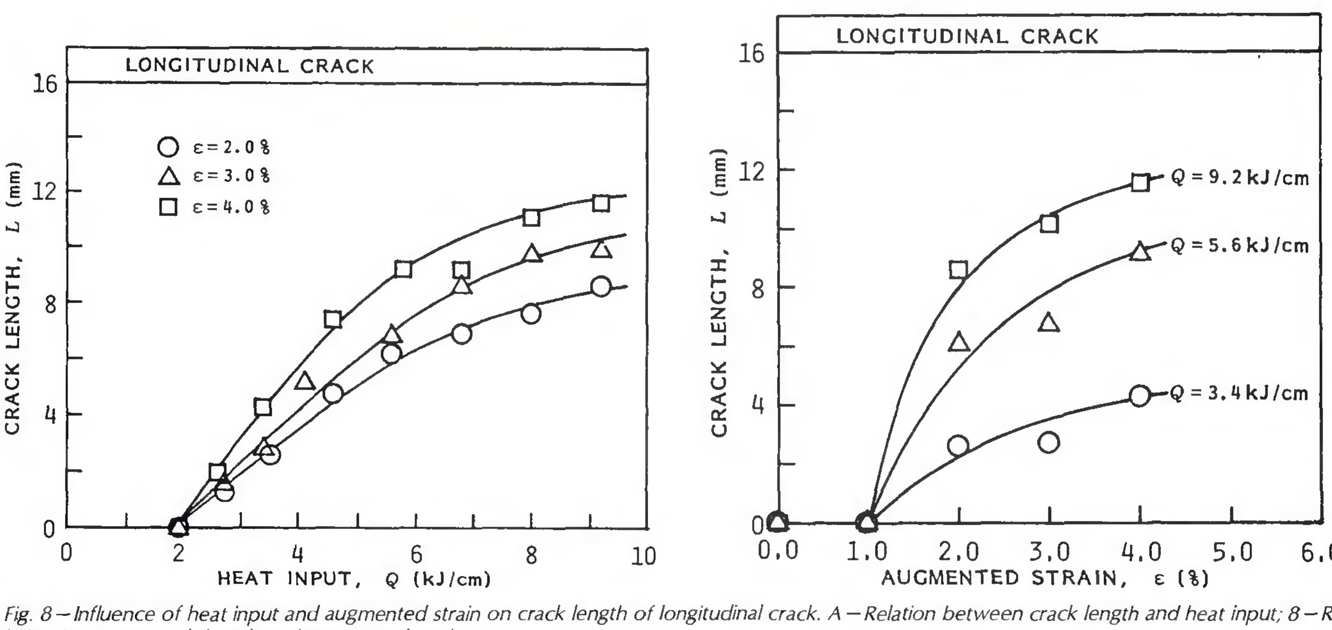

Fig. 8 — Influence of heat input and augmented strain on crack length of longitudinal crack. A — Relation between crack length and heat input; B — Relation between crack length and augmented strain.

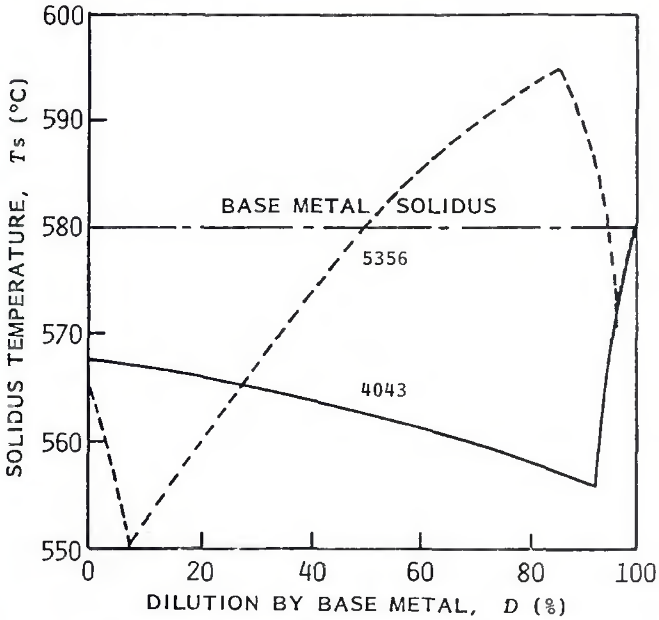

Fig. 9 – Relation between solidus temperature and dilution (after Ref. 2).

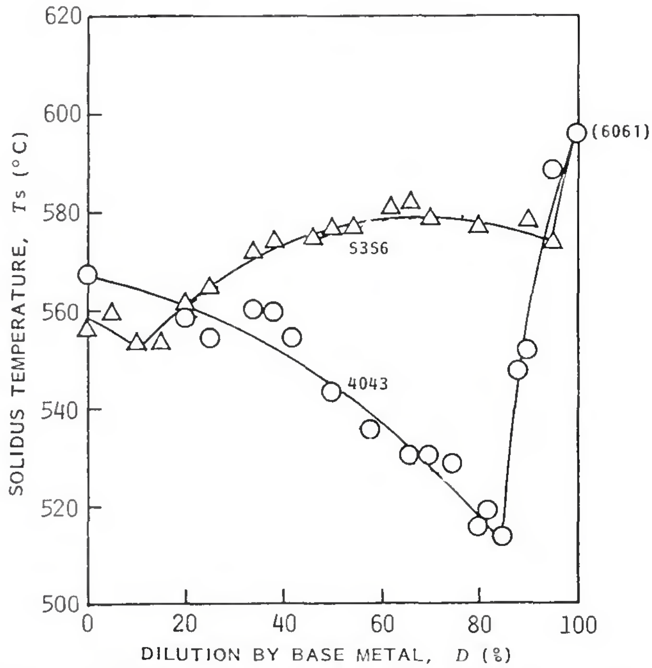

Fig. 10 – Relation between solidus temperature and dilution (experimental value).

pool, but the area of such regions decreased when approaching the crack end. These effects are consistent with results already reported by two of the authors (Ref. 3).

Study on Solidus Temperature

Gittos, *et al.*, obtained the relation shown in Fig. 9 between the solidus temperature Ts and the dilution D by the base metal, using the Al-Mg-Si ternary phase diagram (Ref. 2). Because of intermediate phases formed in this system, in the range of the dilution between 50 and 90%, the predicted solidus temperature of the weld metal was higher than that of the base metal when 5356 filler metal was used. They reported that a crack would be developed along the fusion boundary in this region (they performed the Patch test). When the A6061 alloy was actually GMA welded using 5356 filler metal, longitudinal cracking was observed, but contrary to Gittos, *et al.*, it was not observed that the solidus temperature of the weld metal became higher than that of the base metal (Ref. 3).

This aspect was investigated further, using carefully controlled alloy compositions. Specimens were obtained by melting different ratios of the base metal and the filler metal using a high-frequency induction heating furnace. Using these specimens, the solidus temperature was measured for an average cooling rate between the liquidus and the solidus temperatures of about 30°C/s (54°F/s). The result thus obtained is shown in Fig. 10. In the case of 4043 filler metal, the solidus temperature abruptly decreased from that of the base metal (597°C) to the minimum value 514°C (957°F) at the dilution of 85%, and after that gradually increased with decreases in the dilution. A decrease in the dilution corresponds to a decrease in the heat input in the actual welding. In the case of 5356 filler metal, the solidus temperature initially decreased down to 573°C (1063°F) and after that increased up to 580°C (1076°F) at the dilution of 65%. With further decreases in the dilution, the solidus temperature decreased down to 554°C (1029°F) at the dilution of 15%, and after that tended to increase again.

These relations between the solidus temperature and the dilution are qualitatively the same as those shown in Fig. 9. However, the phenomenon that the solidus temperature in the case of 5356 filler metal is higher for certain dilutions than that of the base metal was not observed. Moreover, the solidus temperature shown in Fig. 10 is generally lower than that shown in Fig. 9. This is considered to be due to the phenomenon that small amounts of minor solute elements greatly affect the solidus temperature in addition to the effects of Mg and Si (Ref. 5).

The dilution actually obtained depended on both heat input and filler metal, as shown in Fig. 11. A similar tendency is observed in each case, that is, the dilution initially increases and after that the slope of the dilution vs. the heat input tends to decrease with further increases in the heat input. When the heat input increased from 1.8 to 9.2 kJ/cm, the dilution increased by about 20%. Generally, the dilution in the case of 4043 filler metal is larger by about 10% than in the case of 5356 filler metal.

Fig. 11 – Relation between dilution and heat input.

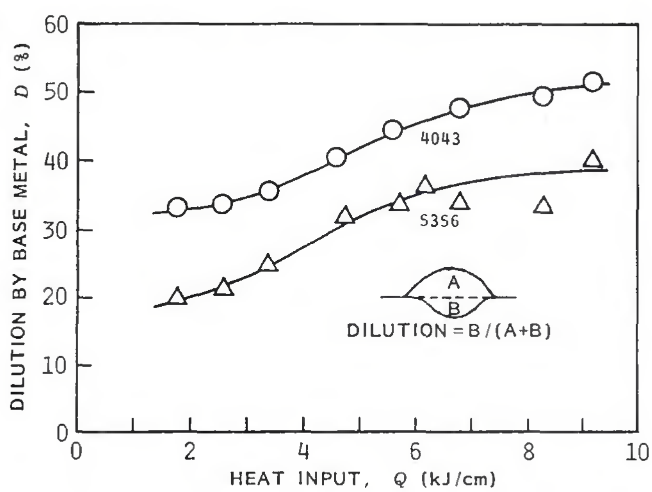

Table 2—Possible Low-Melting Eutectics in Al-Mg-Si Alloys

Eutectics	Melting Temperature (° C)
$Al\text{-}Mg_2Si$	595
Al-Si	579
$Al\text{-}Mg_2Si\text{-}Si$	559
$Al\text{-}Mg_2Si\text{-}(FeMn)_3Si_2Al_{15}\text{-}Si$	<550
$Al\text{-}Mg_2Si\text{-}FeMg_3Si_6Al_8\text{-}Si$	549
$Al\text{-}Mg_2Si\text{-}(CrFe)_4Si_4Al_{13}\text{-}Si$	<550
$Al\text{-}CuAl_2\text{-}Mg_2Si$	514
$Al\text{-}Cu_2Mg_8Si_6Al_5\text{-}CuAl_2\text{-}Si$	507

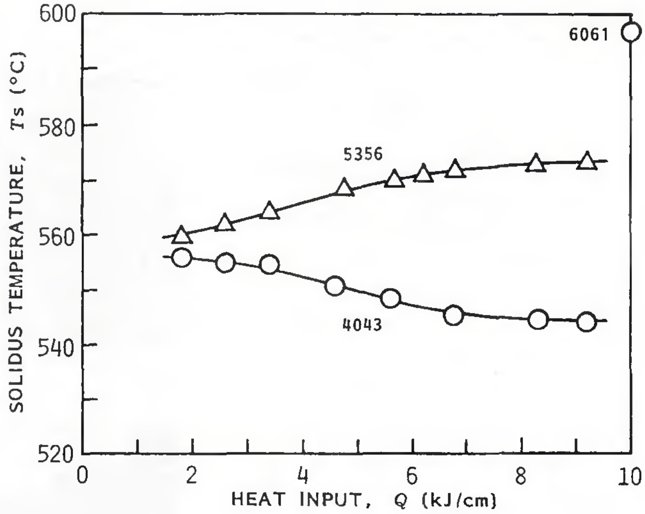

Fig. 12—Relation between solidus temperature and heat input.

Figure 12 shows the relation between the solidus temperature and the heat input, obtained by combining Figs. 10 and 11. The solidus temperature decreased from 556° to 540°C (1033° to 1004°F) in the case of 4043 filler metal, but increased from 560° to 572°C (1040° to 1062°F) in the case of 5356 filler metal with increases in the heat input from 1.8 to 9.2 kJ/cm (4.6 to 23 kJ/in.). This tendency is qualitatively the same as that reported earlier (Ref. 3), but the solidus temperature in Fig. 12 is generally lower by 15° to 20°C (27° to 36°F).

Mechanism of Cracking

As already mentioned, longitudinal cracking is developed along the partially molten zone. This was clearly confirmed to be liquation cracking by the crack surface observation. This phenomenon shows that the weld metal has already solidified when the crack is developed. That longitudinal cracking is devleoped only in the case of 5356 filler metal can be well explained by constitutional liquation (Ref. 3). Table 2 shows the compounds and/or eutectics and their melting points, which have some probability for development in Al-Mg-Si alloys (Refs. 6, 7).

Longitudinal cracking was developed at heat inputs larger than 2 kJ/cm (Fig. 10A), and the weld metal solidus temperature at this heat input is 560°C—Fig. 12. The solidus temperature for the same conditions in the case of 4043 filler metal is 556°C. Longitudinal cracking must occur when the weld metal is essentially solid, with more continuous liquid paths in the partially melted zone. That is, the weld metal welded using 5356 filler metal has already solidified, while liquid remains in the HAZ, and longitudinal cracking is developed. In the case of 4043 filler metal, however, the weld metal has not yet solidified and the cracking is not developed. Considering the small difference in the solidus temperatures between these, and that longitudinal cracking is developed only in the case of 5356 filler metal, the $Al\text{-}Mg_2Si\text{-}Si$ ternary eutectic, which contains 4.6% Mg and 13.2% Si and whose melting temperature is 559°C (1038°F) (Ref. 7), seems to be the most likely to cause the constitutional liquation of all the reactions listed in Table 2. However, according to Mondolfo (Ref. 6), the melting temperature of the $Al\text{-}Mg_2Si\text{-}Si$ ternary eutectic is 550°C (1022°F), *i.e.*, a difference of 9°C (16° F) from the value shown in the *Metals Handbook*. Hence, other eutectics having melting temperatures around 550°C in Table 2 may contribute to the constitutional liquation.

It is difficult to confirm whether these ternary eutectics are actually developed. However, previous work has detected high amounts of solutes such as 2 ~ 7% Mg and 5 ~ 9% Si by analyzing the crack surface using an EDX (Ref. 3). This supports the likelihood that the $Al\text{-}Mg_2Si\text{-}Si$ ternary eutectic is the critical reaction.

When augmented strain is constant, the crack length increases with an increase in the heat input as shown in Fig. 8A, because the region which is heated above the melting temperature widens. Moreover, the crack length increases for the same heat input with an increase in augmented strain, as shown in Fig. 8B, because the crack can be propagated into regions which contain less molten metal.

Transverse Cracking
Features of Cracking

In the case of 4043 filler metal, transverse cracking was observed in the HAZ even in as-welded condition. In the case of 5356 filler metal, however, the cracking was hardly observed as welded, but was observed after machining-off the weld reinforcement.

Figures 13A and B schematically show the features of the cross-section of the weld bead and the cracks in the cases of 4043 and 5356 filler metals, respectively (for $\epsilon = 4.0\%$, Q = 6.7 kJ/cm). The hatched regions represent the cracked regions. These clearly show that the features of the penetration and the crack largely depend on the filler metals. Generally, the width of the weld bead is wider in the case of 4043 filler metal, but the depth of the penetration is almost the

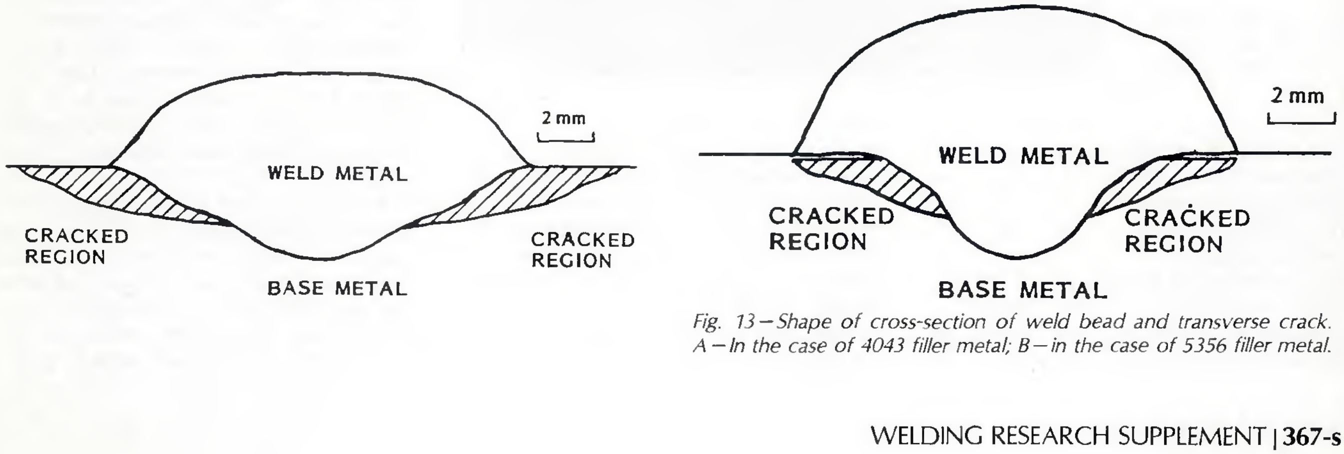

Fig. 13—Shape of cross-section of weld bead and transverse crack. A—In the case of 4043 filler metal; B—in the case of 5356 filler metal.

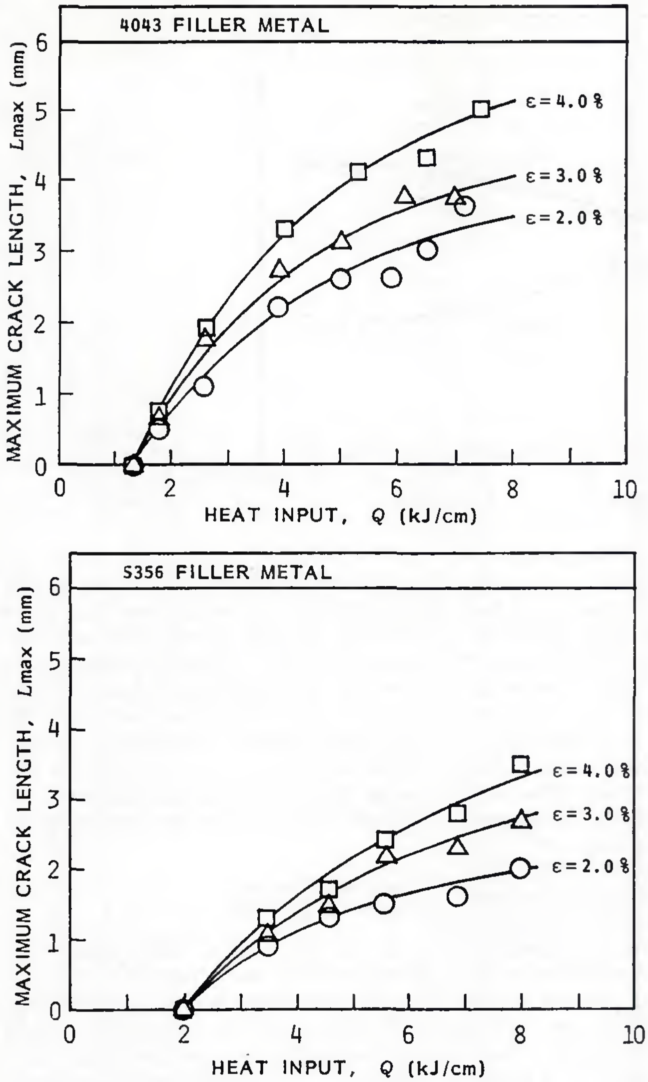

Fig. 14 — Relation between the maximum length of transverse crack and heat input. A — For 4043 filler metal; B — for 5356 filler metal

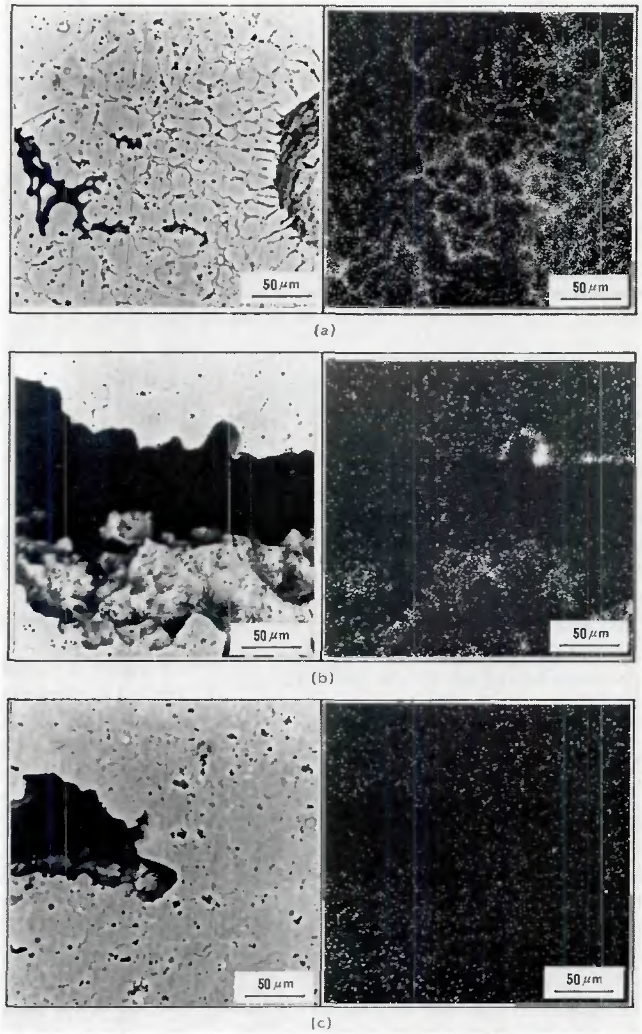

Fig. 16 — SEM images and Si K α images at some locations in Fig. 15. A — At location A; B — at location B; C — at location C.

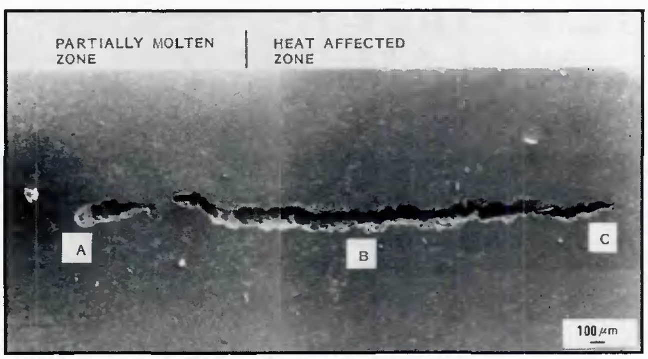

Fig. 15 — SEM image of crack in the case of 4043 filler metal.

same. Therefore, the dilution is larger in the case of 4043 filler metal for the same heat input, as shown in Fig. 11. In the case of 4043 filler metal, most of the crack length is observed on the surface of the base metal region. In the case of 5356 filler metal, however, it is hidden under the weld reinforcement (as is clear from the figure the depth of the penetration is very shallow at this region). The crack in this case was sometimes observed after machining-off the specimen surface of the original base metal a little (less than 0.2 mm). Most of the cracks were propagated from the fusion boundary into the HAZ, though some of the cracks were observed a little apart from the fusion boundary into the base metal.

Factors Affecting Cracking and Their Influences

Figures 14A and B show the relation between the maximum transverse crack length and the heat input in the cases of 4043 and 5356 filler metals. The critical heat inputs at which the cracking began to develop were 1.4 kJ/cm and 1.8 kJ/cm (3.5 kJ/in. and 4.5 kJ/in.), respectively. At heat inputs larger than the critical value, the maximum crack length increased with increases in the heat input. When the heat input was constant, the maximum crack length increased with increases in the augmented strain. No crack was observed at the augmented strain less than 1.0% in both cases.

As is clear when comparing Figs. 14A with 14B, the maximum crack length in the case of 4043 filler metal is about one and a half times longer than in the case of 5356 filler metal for the same augmented strain and the heat input. This shows that the kind of filler metal greatly affects trans-

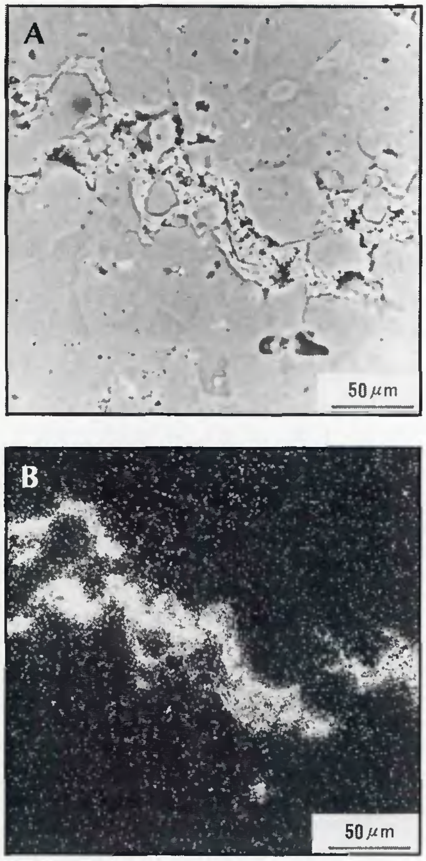

Fig. 17 — Another example of SEM image and Si K α. A — SEM image; B — Si K α image.

Fig. 18 — SEM image of crack in the case of 5356 filler metal.

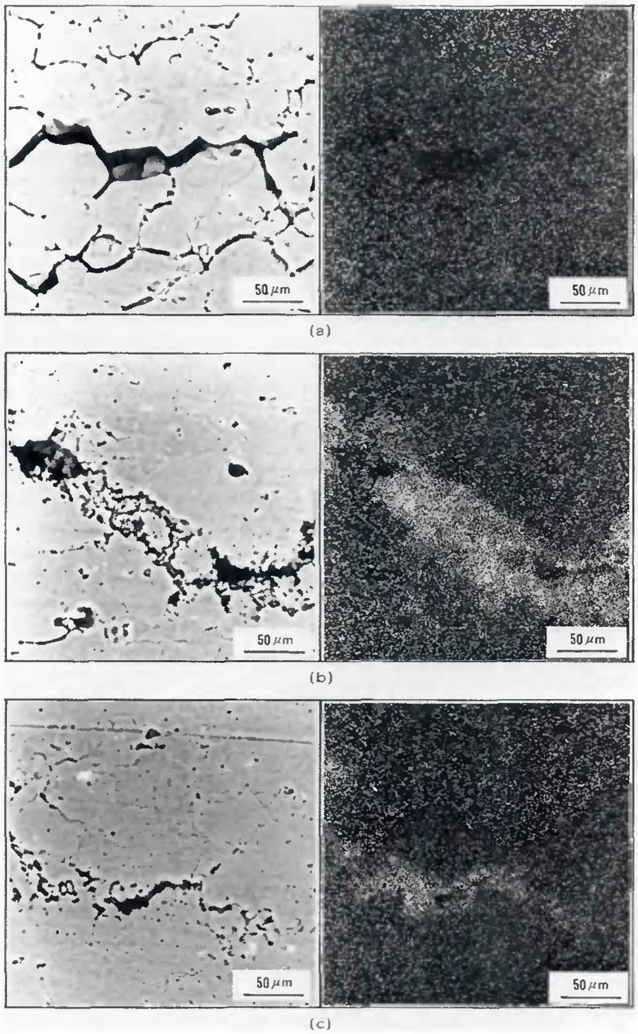

Fig. 19 — SEM images and Mg K α images at some location in Fig. 18. A — at location A; B — at location B; C — at location C.

verse cracking. This phenomenon is qualitatively the same as that reported earlier (Ref. 3).

Figure 15 shows a photograph of the crack using an SEM in the case of 4043 filler metal. The crack is along a grain boundary. Fractographs using an SEM clearly showed that partial melting had occurred. Figures 16A–C show SEM images and Si K α images at locations A, B and C in Fig. 15. The position A belongs to the partially melted zone and much Si is observed here. The position B is nearly halfway along the crack and a high Si concentration is observed near the crack. The position C is the crack end and no marked distribution of silicon is observed in this case. Figure 17 shows another SEM image and Si Kα image at the location of about halfway along a crack different from that shown in Fig. 15. A high concentration of Si is distributed near the crack. No such distribution of Si was observed near grain boundaries where there was no crack. This shows that Si penetrates along grain boundaries when welded using 4043 filler metal. As shown in Fig. 14 A, the maximum crack length increased with an increase in the heat input. A decrease in weld metal solidus temperatures with increased heat input for 4043 filler metal (Fig. 12) may contribute to increased cracking by providing liquid over a longer time (and distance). However, the opposite effect of the heat input on solidus temperature was found for 5356 filler metal (Fig. 12), but cracking still increased with increased heat input — Fig. 14B. This indicates that a decrease in solidus temperature alone does not explain the effect of the heat input. Instead, this phenomenon is due to the fact that the distance corresponding to the difference between liquidus and the solidus temperatures becomes longer with an increase in the heat input.

Figure 18 shows a photograph of transverse cracks obtained when using 5356 filler metal. In this case, many short cracks were observed at locations apart from the fusion boundary besides the main crack. Figures 19A–C show SEM images and Mg K α images at locations A, B and C in Fig. 18. The amount of Mg is less at location A, in the partially melted zone. At locations B, nearly halfway along the crack, and C, the crack end, marked distributions of Mg are observed near the crack. Figure 20 shows another SEM image and Mg K α image halfway along a crack different from that shown in Fig. 18. A high concentration of Mg is observed near the crack. Mg is also considered to penetrate along the grain boundary, similar to the case of Si. However, it is difficult to explain the develop-

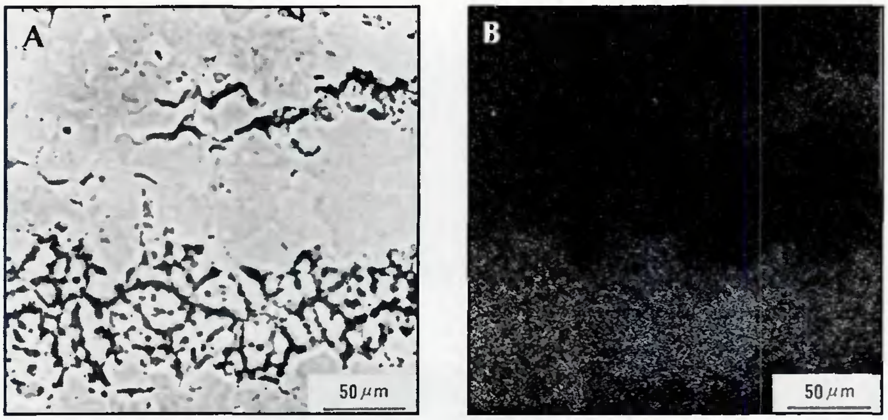

Fig. 20—Another example of SEM image and Mg K α. A—SEM image; B—Mg K α image.

ment of the short cracks shown in Fig. 18 by this mechanism only.

Most of the cracks were hidden under this region of weld reinforcement. As sketched in Fig. 13B, in the case of 5356 filler metal, weld reinforcement generally occurred over a certain width w of macroscopically unmelted base metal. Figure 21 shows the relation between the width w of this region and the heat input. The width w was 1.5 mm (0.06 in.) at the heat input equal to 1.8 kJ/cm with no observable cracks, and increased with increases in the heat input. In Fig. 21, the relation between the maximum crack length and the heat input in the case of $\epsilon = 4.0\%$, shown in Fig. 14B, is also shown. The width w is larger than the maximum crack length in the case of the small heat inputs, and they are almost the same in the case of the heat inputs larger than 8 kJ/cm (20 kJ/in.). Thus, the change of the width w affects the maximum crack length. The reinforcement-added 5356 filler metal exists above the base metal over the region of the width w. This indicates that Mg in the weld reinforcement can penetrate downward over the region of the width w. Hence, it is possible to give a consistent explanation that the short cracks can be developed as observed in Fig. 18. Moreover, it is similarly possible to explain that much Mg is observed near the cracks in Fig. 19 and even near the short cracks in Fig. 20.

Figures 22A and B show an SEM image and Si K α image after a Varestraint test when GMA welding was performed on 99.999% Al with 4043 filler metal. A short crack is observed along the grain boundary, and Si distributes along the crack. This also confirms that penetration of Si or Mg affects transverse cracking.

Conclusions

The main conclusions obtained in this investigation are as follows:

1) The maximum length of liquation cracking of Alloy 6061 in the case of GTA spot welding increased greatly with increases in the grain size from 0.05 to 2 mm, but increased slightly for further increases in the grain size.

2) In the material having the grain size of about 0.05 mm, liquation cracking was developed at the region that was heated above approximately the solidus temperature. When the grain size was coarsened, however, the crack developed to lower temperatures than the solidus temperature.

3) Over a wide range of dilution the solidus temperature in the case of 5356 and 4043 filler metals, the solidus temperature was increased by Si, but decreased by Mg. Generally, the solidus temperature was higher in the case of 5356 filler metal, but in both cases the base metal solidus temperature was still higher.

4) For GMA welding, longitudinal cracking was developed along the fusion boundary only in the case of 5356 filler metal. This phenomenon is explained using the relation between the solidus temperatures and the heat input, plus constitutional liquation in the base metal.

5) Transverse cracking was developed for both of 4043 and 5356 filler metals. The maximum crack length was longer in

Fig. 21—Relation between the width w and heat input.

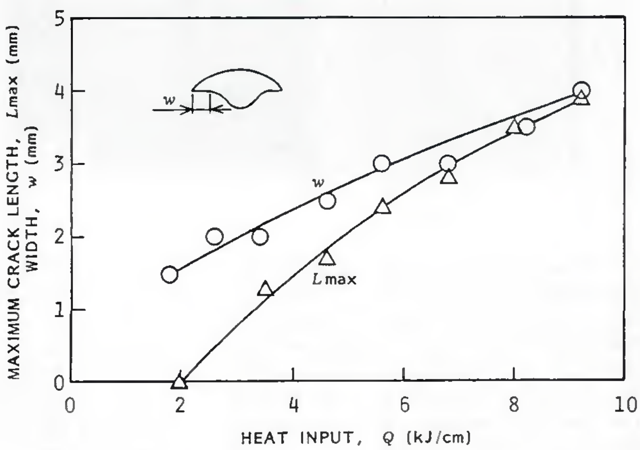

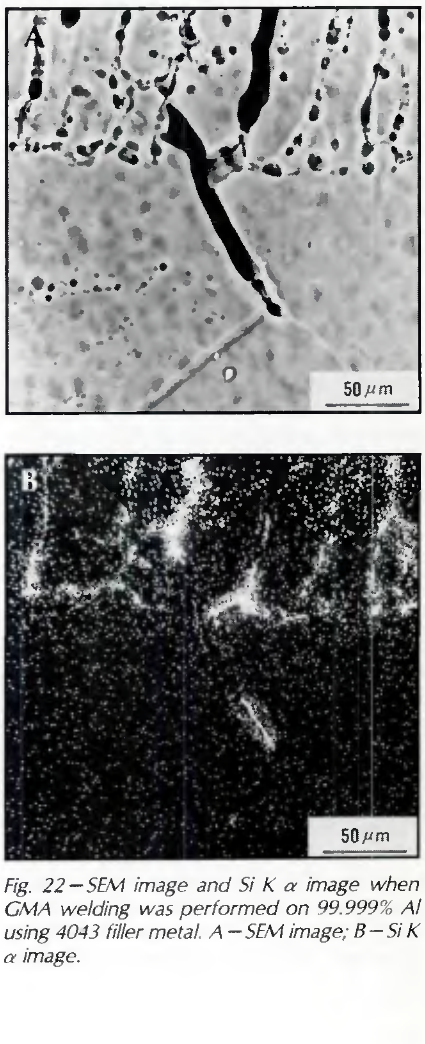

Fig. 22—SEM image and Si K α image when GMA welding was performed on 99.999% Al using 4043 filler metal. A—SEM image; B—Si K α image.

the case of 4043 filler metal.

6) Transverse cracking was observed as welded in the case of 4043 filler metal, but was hidden under the weld reinforcement and observed after machining off the reinforcement in the case of 5356 filler metal.

7) In the case of 5356 filler metal, besides long transverse cracks, many short cracks were observed a little apart from the partially melted zone. The development of these cracks is considered to be caused by Mg diffusing from the weld reinforcement above the cracked region into the HAZ.

References

1. Tsujimoto, K., Sakaguchi, A., Kinoshita, T., Tanaka, K., and Sasabe, S. 1983. HAZ cracking of Al-Mg-Si alloys. IIW Doc. IX-1273, pp. 1–13.
2. Gittos, N. F., and Scott, M. H. 1981. Heat-affected zone cracking of Al-Mg-Si alloys. *Welding Journal* 60(6):95-s to 103-s.
3. Katoh, M., and Kerr, H. W. 1987. Investigation of heat-affected zone cracking of GMA welds of Al-Mg-Si alloys using the Varestraint test. *Welding Journal* 66(9):251-s to 259-s.
4. Kerr, H. W., and Katoh, M. 1987. Investigation of heat-affected zone cracking of GTA welds of Al-Mg-Si alloys using the Varestraint test. *Welding Journal* 66(12):360-s to 368-s.
5. Gustafsson, G., Thorvaldsson, T., and Dunlop, G. L. 1986. The influence of Fe and Cr on the microstructure of cast Al-Si-Mg alloys. *Met. Trans.* 17A(1):45–52.
6. Mondolfo, N. F. 1979. Aluminum alloys: structure and properties. Butterworths: p. 795.
7. *Metals Handbook* Vol. 8. 1973. ASM International, Materials Park, Ohio, p.396.

Invitation to Participate in the Inaugural Meeting of the AWS G2 Committee on Joining Metals & Alloys

This committee was approved at the Spring meeting of the AWS Technical Council. The Scope of the committee is as follows:

> To survey industry groups and identify need for information on joining specific families of alloys. Identify and select specific groups or classes of alloys that are sufficiently alike so that a single standard can be logically prepared on the joining of these metals.
>
> Recruit additional committee and subcommittee members to prepare the selected standards.

The first meeting of the G2 Committee will be held on November 5 and 6, 1990 in Newport News, Va. Anyone interested in attending the meeting should contact Leonard P. Connor of the American Welding Society (800) 443-9353.

WRC Bulletin 352
April 1990

In October 1987, the PVRC Steering and Technical Committees on Piping Systems established a task group on independent support motion (ISM) to evaluate the technical merits of using the ISM method of spectral analysis in the design and analysis of nuclear power plant piping systems.

The results of the task group evaluation culminated in a unanimous technical position that the ISM method of spectral seismic analysis provides more accurate and generally less conservative response predictions than the commonly accepted envelope response spectra (ERS) method, and are reported in this WRC Bulletin. The price of WRC Bulletin 352 is $25.00 per copy, plus $5.00 for U.S., or $10.00 for overseas, postage and handling. Orders should be sent with payment to the Welding Research Council, 345 E. 47th St., Room 1301, New York, NY 10017.

WRC Bulletin 353
May 1990

Position Paper on Nuclear Plant Pipe Supports

This position paper recommends design methods which represent the collective "best methods" of the industry. These enhanced design methods are developed by reviewing the issues that have added to the complexity of design and fabrication of piping systems.

Publication of this report was sponsored by the Task Group on Nuclear Plant Pipe Supports of the Technical Committee on Piping Systems of the Pressure Vessel Research Council of the Welding Research Council. The price of WRC Bulletin 353 is $25.00 per copy, plus $5.00 for U.S., or $10.00 for overseas, postage and handling. Orders should be sent with payment to the Welding Research Council, 345 E. 47th St., Room 1301, New York, NY 10017.

WRC Bulletin 354
June 1990

The two papers contained in this bulletin provide definitive information concerning the elevated temperature rupture behavior of 2¼Cr-1Mo weld metals.

(1) Failure Analysis of a Service-Exposed Hot Reheat Steam Line in a Utility Steam Plant

By C. D. Lundin, K. K. Khan, D. Yang, S. Hilton and W. Zielke

(2) The Influence of Flux Composition of the Elevated Temperature Properties of Cr-Mo Submerged Arc Weldments

By J. F. Henry, F. V. Ellis and C. D. Lundin

The first paper gives a detailed metallurgical failure analysis of cracking in a longitudinally welded hot reheat pipe with 184,000 hours of operation at 1050°F. The second paper defines the role of the welding flux in submerged arc welding of 2¼Cr-1Mo steel.

Publication of this report was sponsored by the Steering and Technical Committees on Piping Systems of the Pressure Vessel Research Council of the Welding Research Council. The price of WRC Bulletin 354 is $50.00 per copy, plus $5.00 for U.S. and $10.00 for overseas postage and handling. Orders should be sent with payment to the Welding Research Council, 345 E. 47th St., Room 1301, New York, NY 10017.